Surface and Frictional Properties of Two-Component Alkylsilane Monolayers and Hydroxyl-Terminated Monolayers on Silicon

Steven G. Vilt, Ziwei Leng, Brandon D. Booth, Clare McCabe, and G. Kane Jennings*

Department of Chemical and Biomolecular Engineering, Vanderbilt University, Nashville, Tennessee 37235

Received: May 22, 2009; Revised Manuscript Received: June 23, 2009

To investigate the effect of chain mobility and functional group exposure on friction, the tribological properties of one-component (pure) and two-component (mixed) alkylsilane monolayers on silicon, with variance in the ratios of long- and short-chain molecules, are presented. The tribological properties of these monolayers were measured with a ball-on-flat tribometer at 9.8 mN load and a speed of 0.1 mm/s. The molecular precursors investigated were *n*-hexyltrichlorosilane (C6), *n*-dodecyltrichlorosilane (C12), *n*-hexadecyltrichlorosilane (C16), *n*-octadecyltrichlorosilane (C18), and *n*-docosyltrichlorosilane (C22). Created from these molecules were the following four mixed monolayers: C6/C18, C12/C18, C16/C18, and C12/C22 in which the ratio of long- and short-chain molecules was varied in order to create different levels of mobility and average chain cant in the upper liquidlike region of the film. For the two-component monolayers, once a critical thickness is reached, the tribological properties were indistinguishable from the pure monolayers although the oleophilicity was much higher for the mixed films. Altering the terminal group of the monolayer to a hydroxyl, however, resulted in an increased coefficient of friction and significant adhesive forces between the monolayer and the stainless steel probe of the microtribometer. This tribological behavior can be explained by the low surface energies of the methyl and methylene groups and the increased adhesion that occurs with hydroxyl-terminated monolayers due to stronger interfacial interactions. Collectively, the results indicate that monolayer thickness and surface energy greatly affect the tribological properties of a monolayer but that molecular mobility within the film and interfacial oleophilicity are less important at these loads and speeds.

Introduction

Driven by the complications of applying liquid lubricants to microelectromechanical systems (MEMS),[1,2] there is an interest in creating solid thin films that possess liquidlike mobilities.[3,4] Two-component, mixed alkylsilane monolayers, in which the two alkysilane components have different chain lengths, represent a way to integrate a mobile, liquidlike layer into a bound film.[1,3,4] The robust siloxane attachment minimizes molecular rearrangement and phase segregation on the surface and ensures a well-mixed structure for these films.[5] Given that the alkyltrichlorosilanes bind with similar efficiency regardless of chain length, the composition and structure of the mixed monolayers can be easily adjusted by varying the chain lengths and concentrations of the two adsorbates.[1,3,5] These mixed monolayers can be viewed as having two distinct regions, a solid lower layer that is densely packed and a more mobile upper layer consisting of only the top portion of longer chain alkylsilanes. Since there are fewer neighboring chains in this upper layer, the chains present in the upper layer must cant from the surface normal into a liquidlike state in order to achieve van der Waals interactions.[1,4] The collapsing of the longer chains exposes the polymethylene backbone of the alkysilane molecules and creates a mixture of CH_3 and CH_2 groups at the mixed monolayer/air interface.[4] The mobile upper layer of the two-component mixed monolayers may prove beneficial for lubrication, as a variety of bound polymer films exhibit lower frictional forces when a liquidlike upper region is incorporated into the film.[6−9]

Recently, the frictional properties of two-component mixed monolayers on silicon have been investigated by two research groups.[1,3,4] Zhang et al.[1,4] used atomic force microscopy (AFM) to compare the nanoscale frictional properties of pure monolayers and mixed monolayers of various short-chain/long-chain ratios. The authors maintained that the mixed monolayers, due to the mobility of the upper region, will provide improved frictional performance if the films possess sufficient packing density to prevent contact between the AFM tip and substrate. More recently, Singh et al.[3] performed a similar study on mixed monolayers but also included microscale friction tests along with the nanoscale AFM tests. The use of a microtribometer offers the ability to test tribological properties at higher forces and speeds while maintaining low to moderate surface pressures. While AFM frictional testing is only single-asperity contact, the microtribometers better mimic the sliding contact area found in many MEMS devices. Singh's[3] AFM friction measurements agreed with the results previously achieved by Zhang,[4] but the microfriction data exhibited different trends than the nanoscale results; at the higher loads, yet lower pressures of the tribometery tests, the mixed monolayers had a higher frictional force than the pure C18 monolayer. Singh et al.[3] maintained that the nN and mN frictional behavior of the mixed monolayers could be explained by the number of monolayer chains in contact with the probe. They proposed that the AFM tip only contacts the long-chain molecules in the upper region, while at the microscale, the counterface ball penetrates the upper region and comes into contact with the short chain components also. This frictional study by Singh et al. was limited to a 1:1 compositional ratio between the short and long chain components.

* To whom correspondence should be addressed. E-mail: kane.g.jennings@vanderbilt.edu. Phone: (615) 322-2707. Fax: (615) 343-7951.

10.1021/jp904809h CCC: $40.75
Published on Web 07/09/2009

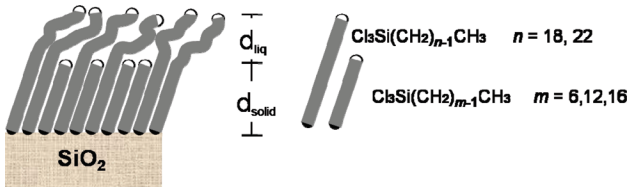

Figure 1. Representation of the molecular structure of mixed alkysilane monolayers. The film can be viewed as having two distinct regions, a solid base layer (d_{solid}) and a mobile upper layer (d_{liq}). Long-chain components of 18 and 22 carbons (n) and short-chain components of 6, 12, and 16 carbons (m) were investigated in this study.

In the present work, we use microtribometry to investigate mixed alkysilane monolayers that contain varying compositional ratios of short- and long-chain molecules. While a mixed monolayer containing a majority of long-chain components would result in a decrease in upper layer fluidity, the resulting enhancement in cohesion of this region through increased van der Waals interactions could provide sufficient support to prevent penetration of the probe while still providing some beneficial mobility. Singh's theory suggests that improved frictional performance would be observed if the probe only contacts the upper region.[3] Zhang's premise is not dependent on tip contact with the lower layer and suggests that improved frictional performance would be observed if probe-substrate interactions can be prevented.[1,4] Furthermore, altering the compositional ratios will result in varying degrees of spacing for the long-chain molecules, which upon collapse of the chains in the outer region, affect the exposure of the methylene backbone at the surface and the resulting oleophilicity of the surface. We have also varied the lengths of the short and long chains to enable investigation of the effects of thickness of the solid base layer and liquid top layer, as well as total thickness of the film, on interfacial friction (Figure 1). We report that the mixed monolayers, once a critical cohesive energy is reached so that probe−substrate interactions can be prevented, have tribological properties that are indistinguishable from the pure, one-component monolayers. At the loads and speeds tested, the coefficient of friction appears to be unresponsive to upper layer mobility and oleophilicity of mixed CH_2/CH_3 surfaces.

The study also includes an investigation into the frictional properties of a hydroxyl-terminated monolayer that was prepared by creating a trichloroacetate monolayer on silicon oxide and then cleaving the terminal ester[10] to form a hydroxyl surface.[11] The hydroxyl monolayer must be created by modification of a pre-existing film because the OH group is synthetically incompatible with a trichlorosilane headgroup. The polar behavior of an alcohol group is vastly different to that of methylene or methyl and provides greater insight into the relationship between functional group exposure and coefficient of friction. Whereas the mixed monolayer results showed frictional insensitivity to oleophilicty, altering the hydrophilicty significantly affected the frictional properties of the monolayers. While there have been tribological investigations involving hydroxyl monolayers created from thiol adsorption,[12−15] our work represents the first report of frictional properties of an OH-terminated monolayer on silicon.

Experimental Section

Materials. *n*-Docosyltrichlorosilane (C22), *n*-hexadecyltrichlorosilane (C16), and *n*-dodecyltrichlorosilane (C12) were purchased from Gelest, *n*-octadecyltrichlorosilane (C18) was purchased from United Chemical Technologies, and *n*-hexyltrichlorosilane (C6) was purchased from Sigma-Aldrich. Trichloroacetyl chloride, trichlorosilane, methanol, undecylenyl alcohol, pyridine, anhydrous tetrahydrofuran, and chloroplatinic acid hydrate were all purchased from Sigma-Aldrich. Hydrogen peroxide (30%, H_2O_2), ethyl acetate, sodium bicarbonate, sodium chloride, and toluene were purchased from Fisher Scientific. Sulfuric acid (H_2SO_4) and hexanes were purchased from EMD Chemicals, Inc. Hydrochloric acid (HCl) was purchased from EM Science. All reagents and chemicals were used as received. Silicon (100) wafers were obtained from Montco Silicon Technologies, Inc.

Synthesis of (1-Trichlorosilyl Undecyl) Trichloroacetate. We prepared (1-trichlorosilyl undecyl) trichloroacetate via a two-step synthesis.[11] Undecenyl alcohol (6.6 mmol) and pyridine (9.9 mmol) were mixed for 30 min under nitrogen and then cooled to 0 °C by submerging the vessel into an ice bath. A 0.5 M solution (14.5 mL) of trichloroacetyl chloride in dichloromethane was then added dropwise to the mixture at 0 °C. The mixture was then stirred for ∼17 h at room temperature to create a dark yellow solution. The solution was then rinsed sequentially with distilled water, 1 M HCl (aq), saturated $NaHCO_3$ (aq), and 5 M NaCl (aq), followed by concentration using a rotary evaporator. The concentrate was then purified by column chromatography using an eluent consisting of 85% hexanes and 15% ethyl acetate, resulting in a product of trichloroacetic acid, undec-10-enyl ester. The terminal enyl group of this compound was then modified using 0.05 g of 0.12 M H_2PtCl_6 in 0.5 mL of dry tetrahydrofuran mixed with 0.5 mL of trichlorosilane and 6 mmol of trichloroacetic acid, undec-10-enyl ester in a N_2 glovebox and then stirred for 4 h under nitrogen at room temperature. The resulting oily dark gray liquid was placed on a vacuum line for ∼5 h and then further purified by vacuum distillation at 180 °C. The resulting product, (1-trichlorosilyl undecyl) trichloroacetate, is a colorless oily liquid. ^{1}H NMR: δ 4.37 (t, 2 H), 1.74 (q, 2 H), 1.57 (q, 2 H), 1.4 (q, 2 H), 1.32 (q, 14 H).

Preparation of Silicon Substrates. Silicon wafers were first cut into 4 cm × 1.3 cm pieces using a diamond-tip stylus. The silicon samples were sequentially rinsed with ethanol, water, and again with ethanol, dried in a stream of N_2, and then sonicated in ethanol for 30 min to displace any remaining contaminants. After sonication, the samples were rinsed sequentially with water and ethanol, dried in a stream of N_2, and placed in piranha solution (14 mL of H_2SO_4/6 mL of H_2O_2) for 30 min to hydroxylate the silicon oxide surface. The piranha-treated substrates were rinsed 3 times by submersion in water. All samples were rinsed once more with DI water, briefly rinsed with ethanol, and thoroughly dried with N_2 before submersion in the precursor solution.

Formation of Alkyltrichlorosilane Monolayers. Pure alkyltrichlorosilane monolayers were formed by immersing the piranha-treated substrates into 1 mM solutions of silane precursors in toluene. The two-component alkytrichlorosilane solutions were prepared individually by mixing in varying microliter volumes of the two alkytrichlorosilanes into 20 mL of toluene in 20 mL glass vials to obtain a total alkytrichlorosilane concentration of 1 mM. After 5 h, the samples were removed from the solution, rinsed in ∼20 mL of toluene for 1 min, sequentially rinsed with ethanol, water, and again with ethanol, dried in a stream of N_2, and then stored in capped glass vials until characterization or testing was performed.

Preparation of Hydroxyl Monolayer. Piranha-treated silicon substrates were immersed in a 1 mM solution of (1-trichlorosilyl undecyl) trichloroacetate in toluene for 5 h. The samples were then removed from the solution, rinsed in 20 mL of toluene for

1 min, sequentially rinsed with ethanol, water, and again with ethanol, and then dried with N_2. The conversion of the trichloroacetate terminal group into a hydroxyl was accomplished by immersion into solution containing 10 mL of deionized water, 10 mL of methanol, and 0.15 g of sodium bicarbonate for 15 min. The resulting hydroxyl-terminated monolayer sample was then sequentially rinsed with ethanol, water, and ethanol, then dried with N_2, and stored in a capped glass vial.

Ellipsometry. Ellipsometric thicknesses were determined from a J. A. Woollam XLS-100 variable-angle spectroscopic ellipsometer. Thicknesses were fit to data taken at 75° from the surface normal over wavelengths from 200 to 1000 nm. The sample was modeled as a 0.5 mm Si substrate with an oxide layer and a Cauchy layer.[16] The thickness of the oxide layer was approximated by measuring a piranha-treated silicon sample obtained fresh each time films were measured. The thickness of the monolayer film was calculated with an index of refraction set to 1.46 (the second Cauchy coefficient was set to 0) and using the software's "normal fit" application. Three separate thickness measurements were taken for each sample. The reported values and errors reflect the average and standard deviation of at least five independently prepared films.

Contact Angle. Contact angles of water and hexadecane were measured with a Rame−Hart manual contact angle goinometer. Advancing and receding contact angles were obtained on both sides of ~10 μL drops with the syringe in the probe droplet during measurements. The reported values and errors reflect the average and standard deviation of at least five independently prepared films.

Microscale Friction Testing. Microscale friction tests were performed with a ball-on-flat microtribotester (Center for Tribology, Inc.) with a two-dimensional (2-D) FVL force sensor. This sensor is capable of measuring forces from 1 to 100 mN in both dimensions with a resolution of 0.01 mN. The probe tip was a 1 mm diameter stainless steel ball firmly glued onto the end of an 8 mm long pin and attached to the sensor via a suspension mounting cantilever. The frictional force tests were performed under a constant load of 9.8 mN and conducted in open air. The sliding speed and the scan length were maintained at 0.1 mm/s and 15 mm, respectively. Five single-pass tests were performed on each sample, with the reported frictional force (F_f) being determined by averaging the forces measured during the five tests. The reported values and errors reflect the average and standard deviation of at least five independently prepared films.

To investigate the affect of adhesion on the tribological performance of the monolayers, friction tests were performed at various loads (9.8, 19.6, 29.4, and 39.2 mN) at a sliding speed of 0.1 mm/s and a scan length of 15 mm. Residual forces (F_o) are a function of the adhesion between surfaces and can be related to frictional force through the modified form of Amonton's law.[17−19] In this model, the friction force (F_f) is defined by

$$F_f = \mu F_n + F_o \quad (1)$$

where μ is the kinetic coefficient of friction, F_n is the normal force, and F_o is the residual force. F_o is the force that is not accounted for by normal spring load and can be estimated by extrapolating frictional force versus normal load plots to zero load. The residual forces for the one-component and two-component alkysilane monolayers were negligible during testing by tribometry (Figure S1 of the Supporting Information); therefore, the reported coefficient of friction values were calculated using the equation

$$F_f = \mu F_n \quad (2)$$

where μ is the kinetic coefficient of friction and F_n is the normal force.

Results

Estimating Composition of Mixed Monolayers Based on Ellipsometric Data. To estimate the compositions of the mixed monolayers, we adopt a method based on thickness that has proven to provide similar results when compared to methods based on attenuation using X-ray photoelectron spectra.[20] We assume that the ellipsometric thickness of the mixed monolayer is a direct function of the binary composition of the monolayer through the equation

$$d_{total} = (1 - x_{lc})d_{sc} + x_{lc}d_{lc} \quad (3)$$

where d_{total} is the ellispometric thickness of the mixed monolayer, d_{sc} and d_{lc} are the ellipsometric thicknesses of the one-component monolayers prepared from short-chain and long-chain adsorbates, respectively, and x_{lc} is the surface mole fraction of the long-chain component in the mixed monolayer. This correlation based on thickness assumes that the index of refraction (1.46) is unchanged for the liquid top layer and solid base layer.

The entire data set for a mixed system was compartmentalized to produce the lowest standard deviation within individual groups, or bins, of similar thickness, with each grouping consisting of at least five independently prepared films. The ellipsometric binning agrees well with the theoretical compositions based on the volumes of trichlorosilane precursors used to prepare the solutions. Categorizing the mixed monolayers based solely on the volumes of the solutions used to prepare the samples was not optimal because of the very small volumes (sometimes as low as 1 μL) used to create the 1 mM solutions, which resulted in inherent experimental error that would occasionally cause erratic and inaccurate groupings. An exception is the C16/C18 mixed system, for which we did rely on the solution concentrations for categorizing these films. The small chain length difference between the C16 and C18 molecules resulted in a narrow range of ellipsometric thicknesses that were often too close to distinguish, given the sensitivity of the ellipsometer (~1 Å). We foresaw difficulty in segregating the C16/C18 data and only attempted to produce three different mixed compositions (target x_{lc} of 0.15, 0.50, and 0.85). We believe the large disparities between the target surface mole fractions are sufficient to overcome any experimental error and provide an accurate reflection of the data set. While we used solution concentrations to group the data for the C16/C18 mixed system, ellipsometric measurements were still used to determine x_{lc} within each group to provide consistency between the various mixed monolayer systems.

Oleophilicty of Mixed Monolayers. As shown in Figure 1, the mobile upper layer of mixed monolayers only contains the longer chain molecules. Depending on the difference in chain length between the short- and long-chain components and the composition of the monolayer, these upper layer chains may collapse into a liquidlike state to achieve favorable van der Waals interactions. The advancing contact angles for hexadecane (Figure 2) clearly demonstrate the effect that chain length

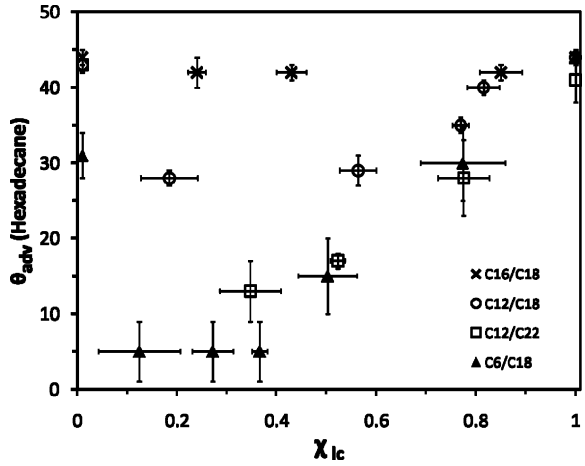

Figure 2. Effect of surface mole fraction of the long-chain component on the advancing hexadecane contact angles for two-component alkylsilane mixed monolayers. Reported values and error bars represent averages and standard deviations, respectively, based on at least five independently prepared films. The pure monolayers consisting of short-chain components ($x_{lc} = 0$) were offset from the *y*-axis for clarity.

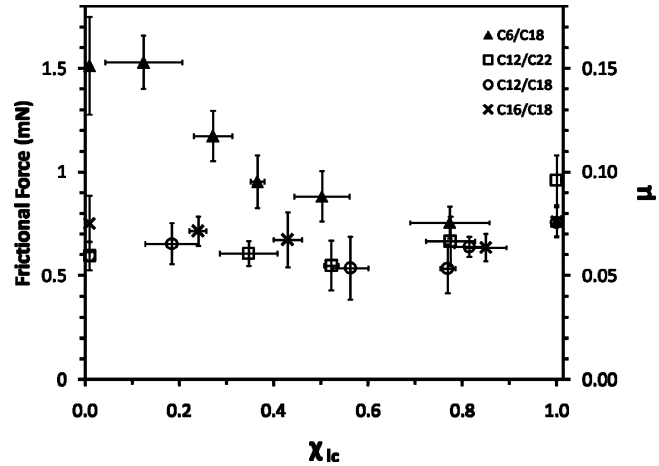

Figure 3. Effect of surface mole fraction of the long-chain component on the frictional properties of two-component alkysilane mixed monolayers. Single-pass tribology tests were performed with a 1 mm diameter stainless steel probe tip at 0.1 mm/s for a length of 15 mm. Reported values and error bars represent averages and standard deviations, respectively, based on at least five independently prepared films. The pure monolayers consisting of short chain components ($x_{lc} = 0$) were offset from the *y*-axis for clarity.

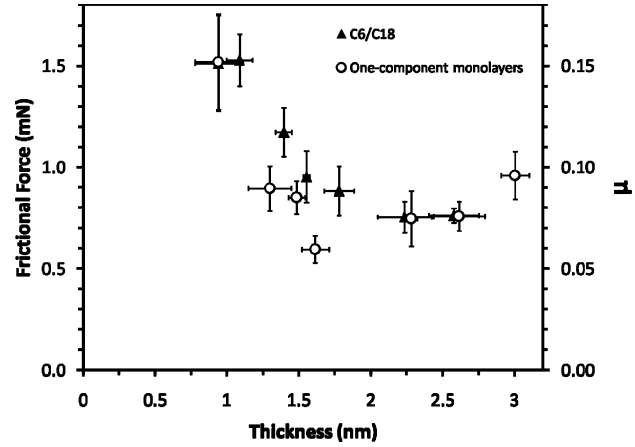

Figure 4. Effect of ellipsometric thickness on the frictional properties of one-component and two-component C6/C18 alkylsilane monolayers. Single-pass tribology tests were performed with a 1 mm diameter stainless steel probe tip at 0.1 mm/s for a length of 15 mm. Reported values and error bars represent averages and standard deviations, respectively, based on at least five independently prepared films. The C6/C18 data points, going from thinnest to thickest, correspond to x_{lc} of 0, 0.12, 0.27, 0.37, 0.50, 0.77, and 1.0. The one-component monolayers studied were C6 (0.94 nm), C8 (1.30 nm), C10 (1.49 nm), C12 (1.62 nm), C16 (2.28 nm), C18 (2.62 nm), and C22 (3.01 nm).

difference and composition have on the oleophilicty of the mixed monolayers. Having a mixed monolayer with a sparse upper layer and a large difference in chain length exposes more methylene groups, as the longer chains would have the molecular freedom and space to cant very close to the lower layer. Molecular collapsing results in an interface consisting of both CH_3 and CH_2 groups, resulting in higher oleophilicty.[1,4,21] Consistent with this molecular interpretation, the C6/C18 monolayers containing a majority of short-chain molecules exhibit the highest oleophilicity. In contrast, a C16/C18 upper layer consists of only two carbons and lacks the length to collapse. The monolayer/air interface would consist of predominantly CH_3 moieties, and therefore, the contact angles for the C16/C18 mixed monolayers vary only a few degrees and are similar to the measurements achieved for organized one-component monolayers.[1]

Advancing water contact angles showed only slight variances across the different mixed and pure monolayers. The one-component monolayers of C12, C16, C18, and C22 all had 110° ± 1° contact angles, which follow past results and signal the presence of a dense methyl surface.[22,23] The one-component C6 monolayer is expected to contain a greater extent of gauche defects[24] than the thicker pure monolayers and therefore exhibits a lower contact angle of 106° ± 2°. The C6/C18 mixed monolayers with a lower density of long chains ($x_{lc} < 0.4$) have advancing water contact angles of 105° ± 1°, which agrees well with a predominantly CH_2 surface.[25] For the other mixed monolayers, where the degree of collapsing is not as extreme and the chain length difference not as large, the water contact angles ranged between 108 and 110°. This result is expected, as previous studies show that water is relatively insensitive to the disorder of the top surface.[21]

Effect of Monolayer Composition on Friction. Measurements of frictional properties for the mixed and one-component monolayers are shown in Figure 3. As discussed in the experimental section, the residual force was shown to be negligible for the one-component and two-component alkylsilane monolayers; therefore, the frictional force and coefficient of friction (μ) values are directly proportional for a constant normal load and can be used interchangeably when comparing the mixed monolayer systems. The C6/C18 system is the only set of films with a clear effect of composition on coefficient of friction, where the coefficient of friction decreases with an increase in C18 composition until a leveling off is reached at a x_{lc} of 0.75. For monolayers with a x_{lc} of ~0.75, the coefficient of friction value of 0.077 ± 0.008 is almost identical to the value obtained for the one-component C18 monolayer (0.076 ± 0.007). To further investigate the behavior of the C6/C18 system, we compared the C6/C18 monolayers with pure monolayers of varying chain lengths (Figure 4). The C6/C18 and one-component data follow the same general trend, a reduction in coefficient of friction for increasing thickness until a plateau is reached. This frictional behavior for the pure monolayers, complete with the minimum at C12, has also been observed in previous studies.[24,26] We believe that the frictional data for one-component and C6/C18 mixed monolayers can be explained by the dependency of coefficient of friction on cohesive energy. One-component films with longer chain lengths

and C6/C18 mixed monolayers with higher percentages of C18 have more intermolecular surface area available for van der Waals interactions and consequently would have higher cohesive energies. The C6 and C8 one-component monolayers and the C6/C18 mixed monolayers with lower percentages of C18 are not sufficiently cohesive to prevent interaction of the probe with the underlying substrate, either through direct contact or noncontact forces. Once a monolayer has sufficient internal stability to prevent interactions between the probe and the substrate, the coefficient of friction remains relatively constant. The trend of thicker (and therefore more cohesive) films providing improved lubrication until a plateau is reached has also been observed by Mino et al.[27] for perfluoroalkylsilane monolayers, Zarrad et al.[28] for CH_3-terminated monolayers prepared from dimethly aminosilane precursors, and us for alkanethiolate monolayers on gold substrates.[15]

In Figure 4, the onset of the C6/C18 plateau in the coefficient of friction occurs at a higher thickness than that of the one-component data. This offset in the plateau is consistent with the mixed monolayers having a liquidlike upper layer. For the C6/C18 films with $x_{lc} \leq 0.50$, the poorly oriented upper layer has a lower density and less cohesion between chains because it contains predominately the collapsed longer chain alkylsilanes. In addition, a C6/C18 film consisting of a majority of C6 molecules will have limited intermolecular surface area to form a dense base layer and offset the concentration of gauche defects that occur near the surface of the substrate.[29] When compared to a one-component film of equal thickness, the C6/C18 mixed monolayer would be less crystalline and would allow easier penetration of the probe, and therefore, a greater thickness is required to prevent probe−substrate interactions.

The mixed monolayers prepared from the other mixed systems (C12/C18, C16/C18, and C12/C22) have short-chain components (C12 and C16) that are significantly longer than C6. The added length of the shorter molecules results in thicker and more robust base layers due to the increased van der Waals interactions so that all have ample internal stability to prevent probe−substrate interaction. Any difference in coefficient of friction for these mixed monolayers would be a result of top layer mobility or changes in oleophilicty due to exposure of CH_2 groups. The coefficient of friction values (Figure 3) for all these two-component monolayers are within a standard deviation of each other regardless of long-chain composition or chain length difference. This insensitivity to composition indicates that surface composition (whether CH_2 or CH_3) and mobility of the top layer chains have little to no effect on the coefficient of friction at the load and speed tested. In evaluating all the results on the friction of mixed monolayers, the critical factor determining the coefficient of friction is interchain cohesion while molecular mobility within the film and exposure of CH_2 groups at the surface are less significant at the loads and speeds tested.

The tribometer results obtained in our study do not compare well with those obtained by Singh et al.[3] Specifically, they reported C6/C18 mixed monolayers ($x_{lc} = 0.50$) to give significantly higher coefficient of frictions than the pure C18 monolayer. Our results show only a slight increase in the coefficient of friction between the C6/C18 ($x_{lc} = 0.50$) and pure C18 film. The differences could be attributed to the variances in testing protocol; while Singh et al. used a smaller load (4 mN vs 9.8 mN), their sliding velocity was 10× greater (1 mm/s vs 0.1 mm/s). Our tribometry study could not be performed with Singh's protocol because the parameters caused erratic and inconsistent data. As a consequence of achieving different tribometry results, the physical interpretation we present differs from the rationalization offered by Singh et al.[3] Using AFM characterization as supporting evidence, Singh et al. reasoned that the microscale loads present in tribometry testing cause the counterface ball to come into contact with both the long and short components and therefore the frictional forces of the mixed monolayers are found to be between the values obtained with the pure monolayers.[3] Our explanation founded on cohesive energy and probe−substrate interactions is based on frictional measurements of four mixed monolayer systems at various compositions and the additional insight, provided by characterization of contact angles and thicknesses, of the physical environment present at the surface of the mixed monolayer.

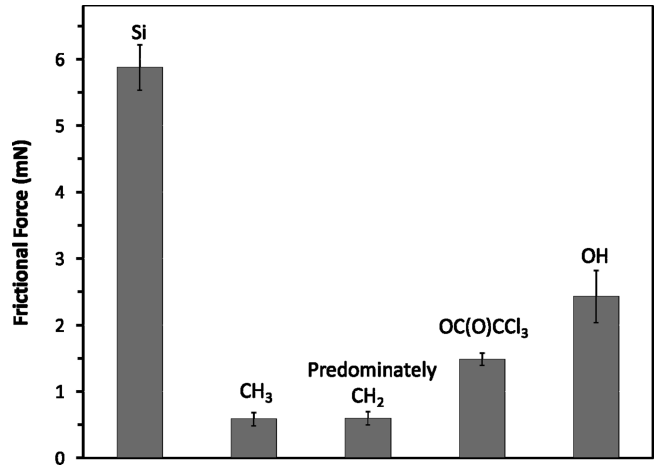

Figure 5. Effect of terminal group on the frictional properties of alkylsilane monolayers. Single-pass tribology tests were performed with a 1 mm diameter stainless steel probe tip at 0.1 mm/s for a length of 15 mm. Reported values and error bars represent averages and standard deviations, respectively, based on at least five independently prepared films. The C12/C22 mixed monolayer group with the lowest mole fraction of long-chain molecules (∼0.35) is classified as the "predominately CH_2 surface."

Surface Energy of Hydroxyl Terminated Monolayer. Methylene and methyl groups allow only weak surface interactions through van der Waals forces. Frictional testing with a hydroxyl-terminated monolayer allows us to compare functional groups with significantly different surface energies, as hydroxyls may participate in hydrogen bonding and other dipole interactions with other surfaces. The hydroxyl monolayers were prepared by forming trichloroacetate-terminated monolayers (advancing water contact angle of 84° ± 1°) from (1-trichlorosilyl undecyl) trichloroacetate and then cleaving the ester terminus into a hydroxyl by hydrolysis. The size of the trichloroacetate limits the packing of the molecules on the surface. By using the bond length between carbon and chlorine and the van der Waal radii of chlorine, the diameter of the trichloroacetate group can be estimated to be at least 5.73 Å, substantially larger than the 4.4 Å diameter of the siloxanol footprint at the substrate surface.[30] Once the trichloroacetate is cleaved into a hydroxyl, the loosely packed monolayer will contain interchain spacing that will allow methylene exposure and results in an intermediate surface energy. The advancing water contact angle (64° ± 1°) is greater than that for densely packed OH monolayers but is almost identical with previous results by Berron et al. for loosely packed hydroxyl-terminated SAMs on gold.[10]

Effect of Terminal Group on Friction. Figure 5 compares different monolayer termini and shows that there is a strong correlation between surface energies and frictional forces. The

CH_3 group presented in Figure 5 refers to a pure C12 monolayer. The C12/C22 group with the lowest mole fraction of long-chain molecules (~0.35) is classified as the "predominately CH_2 surface", as these mixed monolayers represent a methylene-rich surface with a sufficiently thick base layer that prevents probe−substrate contact. The significant collapsing of the upper layer chains and large exposure of methylene groups at the surface is evident by the low hexadecane contact angles (13° ± 3° in Figure 2) achieved for these monolayers. Since the monolayers presented in Figure 5 all have at least 12 atoms along the chain backbone, the effect of thickness on frictional force is eliminated. As noted previously, frictional force (F_f) is insensitive toward methyl (F_f of 0.59 mN) versus methylene (F_f of 0.60 mN) surfaces as these functional groups have very similar interfacial interactions. When functional groups that exhibit higher surface energies are introduced, however, frictional force is increased greatly to 1.49 ± 0.1 mN for the trichloroacetate-terminated monolayer and 2.43 ± 0.4 mN for the hydroxyl-terminated monolayer.

The results in Figure 5 follow expectations, as the higher energy surfaces have a stronger driving force to achieve energetically favorable interactions with the probe. These intermolecular interactions, in addition to capillary forces from physisorbed water vapor, create adhesion between probe and substrate that must be sheared during sliding[31−34] and can increase the linear coefficient of friction and residual force terms in the modified form of Amonton's law (eq 1).[17−19] Adhesive forces can scale at the same order of magnitude as normal force,[32] making the modified form of Amonton's law relevant at the microscale. The trichloroacetate-terminated monolayer showed negligible residual force (Figure S1 of the Supporting Information), indicating that the increase in the coefficient of friction is the primary cause for the higher friction forces. In contrast, the OH-terminated monolayer, in addition to an increase in the coefficient of friction, displayed significant residual forces during tribometer testing (Figure S1 of the Supporting Information).

Conclusion

Collectively, the results for the mixed monolayers and various one-component films indicate that monolayer thickness and terminal group greatly affect the tribological properties of a monolayer, but that molecular mobility within the film and interfacial oleophilicity are less important at the loads and speeds tested. C6/C18 was the only mixed monolayer system that showed a relationship between x_{lc} and coefficient of friction, as the frictional properties remained relatively constant among the other mixed monolayers systems. Once a mixed monolayer has sufficient internal stability to prevent interactions between the probe and the underlying substrate, the tribological properties are indistinguishable from one-component monolayers. Introducing hydroxyl termini into the monolayer, however, resulted in a significant increase in frictional forces, which was attributed mostly to increased adhesion between the probe and film.

Acknowledgment. This work was supported by the Office of Naval Research under grant numbers N00014-06-1-0624 and N00014-07-1-0843 and the State of Tennessee. We thank Dr. Oleg Mazyar and Ben Lewis for insightful discussions.

Supporting Information Available: Figure showing the effect of load force on the tribological performance of the various monolayers. This material is available free of charge via the Internet at http://pubs.acs.org.

References and Notes

(1) Zhang, Q.; Archer, L. A. *J. Phys. Chem. B* **2003**, *107*, 13123–13132.
(2) Alba-Simionesco, C.; Coasne, B.; Dosseh, G.; Dudziak, G.; Gubbins, K. E.; Radhakrishnan, R.; Sliwinska-Bartkowiak, M. *J. Phys.: Condens. Matter* **2006**, *18*, R15–R68.
(3) Singh, R. A.; Kim, J.; Yang, S. W.; Oh, J. E.; Yoon, E. S. *Wear* **2008**, *265*, 42–48.
(4) Zhang, Q.; Archer, L. A. *Langmuir* **2005**, *21*, 5405–5413.
(5) Offord, D. A.; Griffin, J. H. *Langmuir* **1993**, *9*, 3015–3025.
(6) Brown, H. R. *Science* **1994**, *263*, 1411–1413.
(7) Galliano, A.; Bistac, S.; Schultz, J. *J. Colloid Interface Sci.* **2003**, *265*, 372–379.
(8) Gong, J. P.; Kurokawa, T.; Narita, T.; Kagata, G.; Osada, Y.; Nishimura, G.; Kinjo, M. *J. Am. Chem. Soc.* **2001**, *123*, 5582–5583.
(9) Tada, T.; Kaneko, D.; Gong, J. P.; Kaneko, T.; Osada, Y. *Tribol. Lett.* **2004**, *17*, 505–511.
(10) Berron, B.; Jennings, G. K. *Langmuir* **2006**, *22*, 7235–7240.
(11) Seong, J. Ph.D. Thesis, Massachusetts Institute of Technology, Cambridge, MA, 2004.
(12) Sinniah, S. K.; Steel, A. B.; Miller, C. J.; Reutt-Robey, J. E. *J. Am. Chem. Soc.* **1996**, *118*, 8925–8931.
(13) van der Vegte, E. W.; Hadziioannou, G. *Langmuir* **1997**, *13*, 4357–4368.
(14) Flores, S. M.; Shaporenko, A.; Vavilala, C.; Butt, H. J.; Schmittel, M.; Zharnikov, M.; Berger, R. *Surf. Sci.* **2006**, *600*, 2847–2856.
(15) Booth, B.; Vilt, S.; McCabe, C.; Jennings, G. K. *Langmuir* 2009.
(16) Tompkins, H. G.; McGahan, W. A. *Spectroscopic Ellipsometry and Reflectometry: A User's Guide*; John Wiley & Sons: New York, 1999.
(17) Clear, S. C.; Nealey, P. F. *J. Colloid Interface Sci.* **1999**, *213*, 238–250.
(18) Schwarz, U. D.; Allers, W.; Gensterblum, G.; Wiesendanger, R. *Phys. Rev. B* **1995**, *52*, 14976–14984.
(19) Bhushan, B. *Springer Handbook of Nanotechnology*; Springer: Heidelberg, Germany, 2004.
(20) Folkers, J. P.; Laibinis, P. E.; Whitesides, G. M. *Langmuir* **1992**, *8*, 1330–1341.
(21) Laibinis, P. E.; Nuzzo, R. G.; Whitesides, G. M. *J. Phys. Chem.* **1992**, *96*, 5097–5105.
(22) Tillman, N.; Ulman, A.; Schildkraut, J. S.; Penner, T. L. *J. Am. Chem. Soc.* **1988**, *110*, 6136–6144.
(23) Depalma, V.; Tillman, N. *Langmuir* **1989**, *5*, 868–872.
(24) Lio, A.; Charych, D. H.; Salmeron, M. *J. Phys. Chem. B* **1997**, *101*, 3800–3805.
(25) Adam, N. K.; Elliott, G. E. P. *J. Chem. Soc.* **1962**, 2206–2209.
(26) Sambasivan, S.; Hsieh, S.; Fischer, D. A.; Hsu, S. M. *J. Vac. Sci. Technol. A* **2006**, *24*, 1484–1488.
(27) Mino, N.; Ogawa, K.; Minoda, T.; Takatsuka, M.; Sha, S. M.; Moriizumi, T. *Thin Solid Films* **1993**, *230*, 209–216.
(28) Zarrad, H.; Chovelon, J. M.; Clechet, P.; Jaffrezic-Renault, N.; Martelet, C.; Belin, M.; Perez, H.; Chevalier, Y. *Sensor. Actuat. A-Phys.* **1995**, *47*, 598–600.
(29) Hautman, J.; Klein, M. L. *J. Chem. Phys.* **1989**, *91*, 4994–5001.
(30) Ulman, A. *Chem. Rev.* **1996**, *96*, 1533–1554.
(31) Grigg, D. A.; Russell, P. E.; Griffith, J. E. *J. Vac. Sci. Technol. A* **1992**, *10*, 680–683.
(32) Bhushan, B.; Liu, H. W.; Hsu, S. M. *J. Tribol.-Trans. ASME* **2004**, *126*, 583–590.
(33) Beake, B. D.; Leggett, G. J. *Phys. Chem. Chem. Phys.* **1999**, *1*, 3345–3350.
(34) Hayashi, K.; Sugimura, H.; Takai, O. *Appl. Surf. Sci.* **2002**, *188*, 513–518.

JP904809H